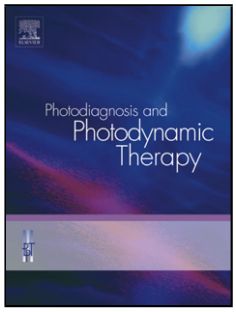

Title: Rapid *ex vivo* examination of Mohs specimens using optical coherence tomography

Authors: D. Rashed, D. Shah, A. Freeman, R.J. Cook, C. Hopper, CM. Perrett

PII: S1572-1000(17)30218-1
DOI: http://dx.doi.org/doi:10.1016/j.pdpdt.2017.06.006
Reference: PDPDT 977

To appear in: *Photodiagnosis and Photodynamic Therapy*

Received date: 24-2-2017
Revised date: 7-5-2017
Accepted date: 11-6-2017

Please cite this article as: Rashed D, Shah D, Freeman A, Cook RJ, Hopper C, Perrett CM.Rapid ex vivo examination of Mohs specimens using optical coherence tomography.*Photodiagnosis and Photodynamic Therapy* http://dx.doi.org/10.1016/j.pdpdt.2017.06.006

Rapid *ex vivo* examination of Mohs specimens using optical coherence tomography

D. Rashed [a, b, c, *] D. Shah[c], A. Freeman[d], R.J. Cook [e], C. Hopper [a, b, f], CM. Perrett [c]

[a]*Head and Neck Unit, University College Hospitals, London, UK.*
[b]*UCL Eastman Dental Institute, Department of Maxillofacial Medicine & Surgery, UCL, London, UK.*
[c]*Department of Dermatology, University College Hospitals, London, UK.*
[d]*Histopathology Department, University College Hospitals, London, UK.*
[e]*KCL Dental Institute, Depts. Oral Medicine & Tissue Engineering & Biophotonics, London, UK.*
[f]*National Medical Laser Centre, Division of Surgery and Interventional Sciences, UCL, London, UK.*

*Corresponding author:
Dr Dara Rashed
UCL/ Eastman Dental Institute, Department of Oral & Maxillofacial Surgery, 256 Gray's Inn Road, London WC1X 8LD, UK
Telephone: 020 3456 1100
Fax: 020 3456 1259
E-mail: d.rashed@ucl.ac.uk

Conflict of interest
None.

Key words:
Mohs micrographic surgery; Basal cell carcinoma; Optical coherence tomography; Ex vivo study

Highlights

- Optical coherence tomography(OCT) is an *in vivo* non-invasive biomedical imaging modality capable of detecting BCCs *in vivo* and *ex vivo*.
- OCT can detect BCCs in *ex vivo* MMS skin samples from different anatomical regions.
- OCT can differentiate between different BCC subtypes.
- OCT could provide a potential role in reducing the number of stages required in Mohs micrographic excision for skin tumours by delineating tumour margins pre-Mohs surgery.

Abstract

Background: Mohs micrographic surgery (MMS) is an effective treatment for certain non-melanoma skin cancers. Optical coherence tomography (OCT) is a biomedical imaging modality that permits high-resolution imaging of the epidermis and dermis with the potential to detect both healthy tissue and tumour. OCT may also provide a means of detecting and differentiating between the various histological subtypes of basal cell carcinomas (BCC) *in vivo*.

Objective: The aim of this prospective *ex vivo* study was to evaluate the efficacy of OCT in recognising healthy and pathological margins of excised BCC lesions and detecting different BCC subtypes.
Methods: Seventy-three subjects with biopsy-proven BCCs on the facial region undergoing MMS were recruited. Narrow clinically healthy margins of the skin surrounding the tumour were included in the excisional biopsy. Biopsies were scanned with the OCT instrument immediately *ex vivo* and processed to obtain horizontal Mohs frozen sections and compared with their corresponding OCT images.
Results: Histopathological analysis of 280 margins showed 232 tumour free margins and 48 tumour-involved margins. OCT showed very good sensitivity (81.2%) and specificity (94.3%) in detecting healthy from tumour-involved margins. OCT accuracy was 93.4%, and the intra- and inter-observer reliability was substantial (Kappa value ranged between 0.63-0.76).
Conclusion: This study shows the accuracy of *ex vivo* OCT in identifying the margin status of BCCs of the head and neck region. Moreover, this modality has demonstrated good capability in distinguishing different BCC subtypes and the potential for *in vivo* in situ diagnostics.

1. Introduction

BCC is the most common non-melanoma skin cancer globally, with an incidence that continues to increase year-on-year [1-3]. Mohs micrographic surgery (MMS) is a precise method in which skin cancers such as BCCs are surgically removed under microscopic margin control [4]. It allows complete margin control during skin cancer removal (CCPDMA – complete circumferential peripheral and deep margin assessment), using horizontal frozen section histology [5,6]. MMS facilitates extirpation of skin cancers with high cure rate and a narrow surgical margin [7,8]. The cure rate with MMS cited by most studies ranges from 97% to 99.8% for primary BCC and 94% for recurrent BCC [9]. However, MMS is generally more time-consuming and labour-intensive than traditional surgery due to the processing of frozen haematoxylin–eosin (H&E) sections.

Accordingly, the combination of MMS with a non-invasive and in real-time modality, such as confocal laser scanning microscopy or OCT, may expedite and facilitate the evaluation of cancer tissue margins as soon as the excision has been performed. The OCT technique has been previously utilised *ex vivo* for the recognition of BCC prior to Mohs horizontal frozen sectioning of excised tissue and showed a low sensitivity (19%) and specificity (56%) [10]. In another recent study, a new high-definition optical coherence tomography (HD-OCT) device (Skintell, AgfaHealthCare, Belgium) utilised 20 excisional biopsies of BCCs to evaluate the feasibility of *ex vivo* HD-OCT in analysing tumour margins compared with the gold standard H&E [11]. The authors reported a higher sensitivity (74%) and specificity (64%) compared with Cunha *et al*. study [10].

The objective of this prospective clinical *ex vivo* study was to examine the accuracy of the OCT instrument against Mohs frozen section histology in recognising the healthy and tumour-laden margins of excised BCC lesions in the facial region. The ability of OCT in distinguishing various BCC subtypes was also assessed.

2. Patients and methods

2.1. Patients

Seventy-three subjects with biopsy-proven BCC undergoing MMS at University College London Hospitals Dermatology Department were selected and recruited for the current study. Inclusion criteria

included patients above 18 years old. Additional inclusion criteria were clinically apparent lesions that had not undergone any previous treatment modality including topical therapeutic agents such as imiquimod, 5-fluorouracil or photodynamic therapy. The study protocol was approved by the NRES (national research ethics service) Committee London-Dulwich (12/LO/0371) and informed consent was obtained from all patients.

2.2. Methods/study designs

Subjects with biopsy-proven BCCs on the facial region referred for MMS were prepared by mapping the boundary of the lesion with the naked eye using a surgical skin marker pen. A 1-2mm margin of clinically apparent healthy skin around the tumour was included in the Mohs extirpation. Following the first and possible further stages of MMS, the OCT instrument was used for immediate *ex vivo* scanning and capturing images of the margins of the specimen to verify its status. Specimens were placed on a piece of gauze with the epidermis facing upwards, and subsequently onto a Petri dish. Four margins per biopsy tissue were studied (total number 292). The four locations scanned were at the 3, 6, 9, and 12 o'clock positions. Scanning was initiated from the periphery towards the centre for each location (Fig. 1). For biopsies larger than 6mm in diameter, each margin was scanned several times to cover all areas from periphery towards the centre using assembled composite images. As part of our routine practice the biopsies were then processed for horizontal frozen sections by a Mohs histotechnician after image acquisition of the specimen using the OCT instrument. The acquired OCT images of the specimen margins were then compared with their corresponding H&E sections.

Two investigators (D.R. & C.H.) independently examined and compared the OCT images with the H&E slides to ascertain whether the margins were clear or involved. The margin status of the Mohs sections was determined by a Consultant Mohs surgeon (C.P.) and a Consultant Histopathologist (A.F.). Assessment was conducted according to WHO guidelines. The criteria employed to identify and rate a margin as negative (tumour-free) were the presence of an intact dermo-epidermal junction (DEJ) with normal overlying epidermis layer and underlying dermis layer (Fig. 2), whereas for identification of a BCC in the positive margin (tumour-laden margin), at least one of the following criteria was required: presence of honeycomb-like aggregates (lobules of small tumour), dark rounded areas (islands of tumour nests), or plug-like signal-intense structures (dense tumour clusters) with or without breached DEJ (Fig. 3). The two assessors re-examined all the OCT images after 5 weeks to determine intra-observer differences, whereas inter-observer agreement was obtained by comparing the assessors' findings.

2.3. Optical coherence tomography oral instrument

In this study, we used a recent variant (OCT oral instrument, version 2.1) of a commercial frequency domain swept source OCT dermatological instrument (SS-OCT, VivoSight® Michelson Diagnostics Ltd, version 2.0, Orpington, Kent, UK). The OCT oral instrument features an extended optical path relaying the imaging aperture into the oral cavity and imaging through a final right angle mirror, for improved intra-oral soft and hard tissue imaging accessibility (Fig. 4).

The light source utilised by this instrument is Santec HSL-2000 swept laser with a centre wavelength of 1305± 15nm, and sweep range of 150nm. VivoSight® utilises four staggered OCT sources and is ideally suited to applications in scattering media such as skin and tumour tissue. In standard configuration, the instrument is reported to achieve axial and lateral resolutions of < 10μm over a depth range of 2mm and image width up to 6mm [12]. The tissue penetration depth is around 1-2mm depending on the optical absorption and scattering properties of the tissue being imaged [12]. In addition, the system can generate both two- and three-dimensional images by reconstruction of serial two-dimensional slice data [12].

2.4. Statistical analysis

The effectiveness, sensitivity, specificity and overall accuracy of OCT (not accounting for chance agreement) were calculated in Excel, Microsoft Office 2003 according to the data provided by both investigators. Kappa statistics were calculated in '2015 GraphPad Prism Software' to assess the agreement between the readers and interpreted as poor if $\kappa < 0.00$, slight if $0.00 \leq \kappa \leq$ to 0.20, fair if $0.21 \leq \kappa \leq$ to 0.40, moderate if $0.41 \leq \kappa \leq$ to 0.60, substantial if $0.61 \leq \kappa \leq 0.80$, almost perfect (or excellent) if $\kappa > 0.80$ according to Landis & Koch [13].

3. Results

The mean age of patients was 67.5 years (range 26–96). There were 39 male and 34 female subjects. BCC lesions were mainly of mixed subtypes (two or more than two subtypes) in 27 cases, followed by nodular (20), micronodular (11), infiltrative (8) and superficial subtype (7) (Figs. 7-9). Cheek (17) and nose (17) were the commonest locations for the BCC lesions, followed by forehead/temple (14), periorbital area (10) and scalp (10), whilst ears (3) and lips (2) were the least common locations (Table 1).

Histopathological analysis of 292 margins showed 232 tumour free margins and 48 tumour-involved margins. Twelve margins were excluded because of distortion (severe artefact) during histopathologic processing and poor quality OCT images.

The intra-observer agreement was substantial (Kappa statistic= 0.76). Furthermore, the degree of concordance between both readers (inter-observer agreement) was also substantial, although the kappa statistic was a little lower (Kappa statistic= 0.63).

4. Discussion

The results of this study demonstrated that epidermis, dermis (papillary and reticular layers) and DEJ can be clearly identified with OCT. The loss of normal characteristic skin layers seen in BCCs can be detected on OCT images.

The OCT penetration depth in the current study was limited to a maximum of only 1-1.5mm, which is adequate to visualise both the epidermis and dermis layers where most of the pathological changes are seen. However, BCCs and nests that penetrate deeper (2mm onwards) in the lower reticular dermis or subcutaneous layers are beyond the scope of OCT, reflecting its relatively shallow penetration depth ability. The lateral and axial resolution of 10-15μm would not permit single cell detection. Nevertheless, one of the advantages of OCT over confocal laser scanning microscopy (CLSM), which has non-invasively achieved 1μm resolution with a 200-400μm field of view in near real time, albeit with a shallow penetration depth of up to 500μm [14-19], is the possibility of microanatomical structure analysis to a depth of 1500μm. On this basis, identification of abnormalities that extend from the papillary dermis to the upper reticular dermis seems possible. This involves regions where the epidermis has slight thickness, in which assessment of part of the reticular epidermis can be achieved [20,21].

In the current study, OCT images of nodular and micronodular BCC subtypes where characterised by distinctive circular or oval tumour aggregate formation in the epidermal and upper dermal layers. While the infiltrative subtype OCT images showed tumour nests much smaller in width (the majority were two cells in width), with jagged contours giving the appearance of either straight or curved small spikes and strands of tissue. The superficial BCC growth pattern in the OCT images appeared as an atypical basaloid proliferation parallel to the long axis of the epidermal layer and showed little or no penetration into the dermal layer. The OCT instrument may in the future, with further refinement, prove useful in differentiating the different BCC subtypes.

In this study BCCs showed characteristic features on examination with the OCT instrument, although some OCT images were difficult to interpret due to lack of sufficient contrast (image quality) and resolution. In such instances it was challenging to define the borders of the nests and strands of the BCC subtypes and differentiate them from the adnexal structures (particularly sebaceous glands), and shadow artefacts resulting from hyperreflectivity of the keratinised or ulcerated outer surface layers of the skin. In concordance with Cunha *et al*. study [10], previously described OCT features of BCC including honeycomb-like signal-free structures, large plug-like signal-intense structures and prominent signal-free cavities in upper dermis [22] were not identified in our study. However, adnexal structures were identified, although often difficult to differentiate from tumour in some specimens.

Another prospective study which used *in vivo* OCT to examine 43 BCCs, reported the capability of *in vivo* OCT in imaging the altered architecture of skin layers and histological correlates of BCC. The BCC tumour nests in its different shapes, i.e. lobules, islands, and infiltrating strands appeared similar in OCT images and histopathology pictures, regardless of the tumour subtype [22]. Our study showed similar results with regard to detection of disorder in skin layer architecture in the presence of BCC but at the same time recognised dissimilar BCC nests, although our clinical study was *ex vivo* in nature and utilised a different OCT system.

OCT sensitivity and specificity compared with Mohs histopathology for distinguishing BCC margins were 81.2% and 94.3% respectively. The positive predictive value was 80.5% and the negative predictive value was 96.1%. Prevalence was 0.16, OCT accuracy was 93.3% and the Kappa statistic was 0.76 (95% confidence interval (CI): from 0.65 to 0.87) (substantial agreement). Positive likelihood ratio (LR+) was 22 and negative likelihood ratio (LR-) was 0.24, suggesting that OCT instrument is useful and provides evidence to support our hypothesis. However, the investigators encountered difficulties in interpreting some of the tumour margins, either due to OCT limited penetration depth or appearance of dark (hyporeflective) structures, which resulted in some false positives and negatives, respectively (Figs. 5 and 6).

In our study, identification of cutaneous tumour resection margins with OCT was demonstrated. Utilising any optical non-invasive diagnostic method in order to improve the accuracy of excisions might confer an advantage to patients by preserving as much normal tissue as possible, particularly in the head and neck region where function and cosmesis are of important as well as reducing the number of surgeries. However, the current OCT instrument technology needs refining (by improving image resolution and penetration depth) in order to optimise its use in the clinical setting and obtain trustworthy data especially for lesions penetrating deeper into the tissue (exceeding 2mm).

Facial cutaneous malignancies can extend below the surface, and indeed more so than clinical examination might suggest. Such lesions may also have indistinct clinical margins, requiring several stages of Mohs surgery to achieve complete clearance. In a recent study, a laboratory bench-top OCT microscope with similar 4 beam construction and resolution (EX1301; Michelson Diagnostics, Orpington, Kent, UK) was compared with conventional frozen-section histopathology for visualising BCC during MMS. In a study of 38 patients, the authors noted that on the average, the mean time to produce one OCT image was 7 minutes, whereas 20-40 minutes were required to produce H&E sections [10]. However, our hand-held oral probe OCT system was faster in comparison, with an image acquisition times of approximately 15-30 seconds per margin, i.e. 2 minutes per lesion if four locations were scanned. Therefore, the real-time intraoperative OCT system is unlikely to lengthen the time of the surgical procedure and will provide near-instantaneous imaging feedback to the operator.

It is unlikely that intraoperative OCT imaging will identify occult deeper tumour areas, as presently the greatest depth of penetration of OCT imaging is around 2mm. Therefore, in iceberg-shaped tumours for instance, resection margin analysis would be difficult. The majority of false negative readings in the current study were related to this phenomenon.

Notwithstanding that, the real-time morphological information attained by OCT scanning, vis-à-vis the epidermal and dermal layers in addition to the ability to demonstrate the junction between these two layers, makes it a promising mapping instrument. In the most recent pilot study performed by Maier *et al*. [11], a new high-definition optical coherence tomography (HD-OCT) system was used to image 20 biopsies of BCC lesions *ex vivo* in horizontal (en face) and vertical (slice) imaging modes. These OCT images were then compared with the gold standard histopathology. The authors reported a higher sensitivity (74%) and specificity (64%) compared with a study by Cunha *et al.*, which reported 19% and 56% sensitivity and specificity respectively [10].

Although our study shows the advantage of rapid *ex vivo* OCT scanning of the specimen margin, one of the main drawbacks is that we scanned and assessed only four margins (3,6,9, and 12 o'clock positions) per specimen. Areas in between the four scanned locations were not imaged. In future studies, this could be overcome by scanning the entire margin. Although this would increase scanning time to circa 3-6 minutes, it still compares favourably with the processing time for Mohs frozen sections.

5. Conclusion

Our data in this study show the accuracy of the OCT instrument in identifying the margin status of BCCs located in the head and neck region, albeit with some false positive and negative margins of the excisional biopsies examined. The OCT system demonstrated good correlation with histopathological analysis. Furthermore, OCT was successfully employed to differentiate between BCC subtypes. Nevertheless, tumour identification was more challenging in thicker tumours exceeding 2mm in depth as they extend beyond the OCT signal depth. Eventually, intraoperative OCT imaging may allow a reduction in the number of stages of MMS and further optimise preservation of normal tissue.

At this moment in time, biopsy and subsequent histopathologic investigation remains the gold standard technique in diagnosing skin malignancies. However, refinement of the existing non-invasive laser-based modalities, for example CLSM, OCT etc. in terms of resolution and penetration depth may improve the early detection of suspicious lesions in the head and neck region and reduce the number of surgical procedures to which patients are subjected.

Funding sources

This research did not receive any specific grant from funding agencies in the public, commercial, or not-for-profit sectors.

Acknowledgments

We thank the staff of dermatology department at UCLH for their help and cooperation.

References

[1] A.A. Marghoob, Basal and squamous cell carcinomas. What every primary care physician should know. Postgrad Med. 102 (1997) 139–54.

[2] D.S. Rigel, R.J. Friedman, A.W. Kopf, Lifetime risk for development of skin cancer in the U.S. population: current estimate is now 1 in 5. J Am Acad Dermatol. 35 (1996) 1012–13.

[3] S.A. Holme, K. Malinovszky, D.L. Roberts, Changing trends in nonmelanoma skin cancer in South Wales, 1988–98. Br J Dermatol. 143 (2000) 1224–9.

[4] F.E. Mohs, Chemosurgery: a microscopically controlled method of cancer excision. Arch Surg.42 (1941) 279–95.

[5] National Comprehensive Cancer Network. National Comprehensive Cancer Network clinical practice guidelines in oncology (NCCN Guidelines): Basal cell and squamous cell skin cancers, Fort Washington, Pennsylvania, 2006.

[6] N. Dhingra, A. Gajdasty, J.W. Neal, *et al*., "Confident complete excision of lid-margin BCCs using a marginal strip: an alternative to Mohs surgery". The British Journal of Ophthalmology 91 (6) (2007) 794–6.

[7] S.H. Bentkover, D.M. Grande, H. Soto, *et al*., "Excision of head and neck basal cell carcinoma with a rapid, cross-sectional, frozen-section technique". Archives of Facial Plastic Surgery 4 (2) (2002) 114–9.

[8] T.J. Minton, "Contemporary Mohs surgery applications". Current Opinion in Otolaryngology & Head and Neck Surgery 16 (4) (2008) 376–80.

[9] G.R. Mikhail & F.E. Mohs, Mohs micrographic surgery. Philadelphia: W.B. Saunders (1991) p. 13.

[10] D. Cunha, T. Richardson, N. Sheth, *et al*., Comparison of *ex vivo* optical coherence tomography with conventional frozen-section histology for visualizing basal cell carcinoma during Mohs micrographic surgery. Br J Dermatol. 165 (2011) 576–580.

[11] T. Maier, D. Kulichova, T. Ruzicka, C. Kunte, C. Berking, *Ex vivo* high-definition optical coherence tomography of basal cell carcinoma compared to frozen-section histology in micrographic surgery: a pilot study. J Eur Acad Dermatol Venereol. 28 (1) (2014) 80-5.

[12] Www.michelsondiagnostics.com. https://vivosight.com/about-us/product/#technology (accessed 29.01.17).

[13] J.R. Landis & G.G. Koch, The measurement of observer agreement for categorical data. Biometrics 33 (1977) 159-174.

[14] M. Rajadhyaksha, M. Grossman, D. Esterowitz, *et al*., *In vivo* confocal scanning laser microscopy of human skin: melanin provides strong contrast. J. Investig. Dermatol. 104 (1995) 946-952.

[15] M. Rajadhyaksha, S. Gonzalez, J. M. Zavislan, *et al*., *In vivo* confocal scanning laser microscopy of human skin. II. Advances in instrumentation and comparison with histology. J. Investig. Dermatol. 113 (1999a) 293-303.

[16] M. Rajadhyaksha, R. R. Anderson, R. H. Webb, *et al*., Video-rate confocal scanning laser microscope for imaging human tissues. in vivo. Appl. Optics 38 (1999b) 2105-2115.

[17] W. M. White, M. Rajadhyaksha, S. Gonzalez, *et al*., Noninvasive imaging of human oral mucosa *in vivo* by confocal reflectance microscopy. Laryngoscope 109 (1999) 1709-1717.

[18] T. Collier, P. Shen, B. de Pradier, R. Richards-Kortum, Near real time confocal microscopy of amelanotic tissue: dynamics of aceto-whitening enable nuclear segmentation. Optics Express 6 (2000) 40-48.

[19] T. Collier, A. Lacy, R. Richards-Kortum, *et al*., Near real-time confocal microscopy of amelanotic tissue: detection of dysplasia in *ex vivo* cervical tissue. Academic Radiol. 9 (2002) 504-512.

[20] K. Sauermann, S. Clemann, S. Jaspers, *et al*., Age related changes of human skin investigated with histometric measurements by confocal laser scanning microscopy *in vivo*. Skin Res Technol. 8 (1) (2002) 52-6.

[21] K. Sauermann, T. Gambichler, S. Jaspers, *et al*., Histometric data obtained by *in vivo* confocal laser scanning microscopy in patients with systemic sclerosis. BMC Dermatol. 6 (2002) 2:8.

[22] T. Gambichler, A. Orlikov, R. Vasa, *et al*., *In vivo* optical coherence tomography of basal cell carcinoma. J Dermatol Sci. 45 (2007)167-73.

Fig. 1. Diagram shows the direction of OCT scanning (blue arrows) from the periphery towards the centre of the excisional specimen at 3,6,9 and 12 o'clock positions.

Fig. 2. True negative margin from a basal cell carcinoma (BCC) lesion. Both histopathology (H&E) & optical coherence tomography (OCT) images (A & B) reveal no tumour cell nests, intact dermo-epidermal junction (DEJ) and homogenous dermis (D). EP= epidermis; HF= hair follicle; SeG= sebaceous gland.

Fig. 3. True positive margin from a tumour-laden resection margin of a nodulocystic (or nodular) BCC lesion. Both images (A & B) show tumour nests and cystic changes in the papillary & reticular dermis layers (PD & RD), with breach in continuity of DEJ in some areas. The convex white line on top of OCT image indicates the glass window of the OCT oral probe.

Fig. 4. OCT oral instrument probe (A) and dermatology probe (B).

Fig. 5. False positive margin of a BCC lesion. H&E image (A) reveals intact DEJ with no tumour nests, whereas OCT image (B) shows no clear distinction (DEJ) between epidermal and dermal layers and the presence of numerous large hypo-reflective (low scattering) tumour-like round structures in both epidermal and dermal layers.

Fig. 6. False negative margin of a BCC resection margin. H&E picture (A) showing deep tumour nests of both nodular & micronodular subtypes in the reticular dermis, which is clearly beyond OCT penetration depth capability. OCT scan (B) revealing distinct epidermis, intact DEJ and homogenous dermis.

Fig. 7. Superficial BCC shown in both histology slide & OCT image (A & B). Note the downward growth of basal cell layer of the epidermis (arrows) without a breach in the continuity of DEJ.

Fig. 8. Mixed nodular & micronodular BCC subtypes shown in both histology slide & OCT image (A & B). Red arrows indicate nodular nests, whereas white arrows indicate micronodular basaloid nests. Palisading (halo-like region) is obvious around the ovoid basaloid nest (round brackets), which is due to the presence of either mucin secretion within a cleft or nuclear material that has been suggested to cause hypo-reflectivity (low scattering properties). The suggested 'halo' consists of irreflective circumsriptive thin line. SwG (sweat glands) can be seen in the histopathological image, which is beyond OCT penetration depth ability.

Fig. 9. Infiltrative type BCC shown in both H&E & OCT pictures (A & B). Note the dramatic alteration of the morphology of both epidermal and dermal layers in the region where the BCC nests reside in. Variability in shape & size of tumour cell nests is noticeable with jagged contours in comparison with other BCC subtypes.

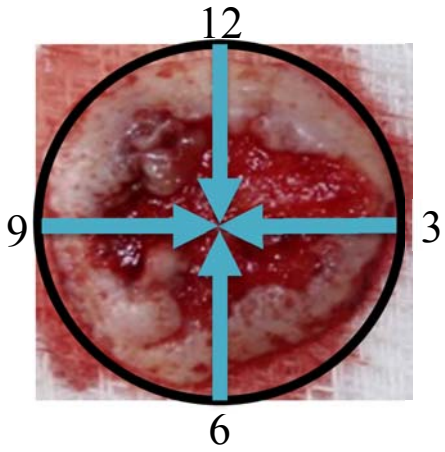

Fig. 1.

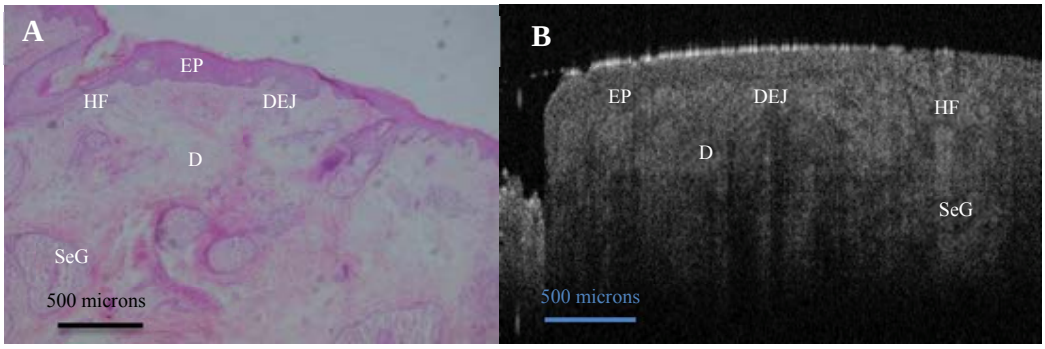

Fig. 2.

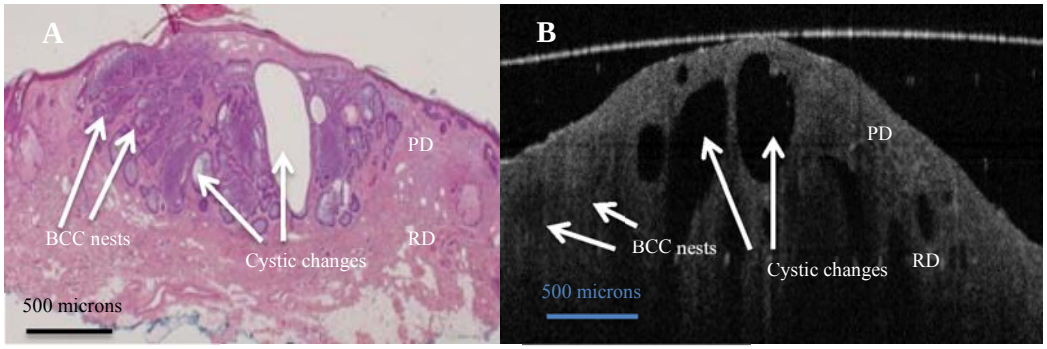

Fig. 3.

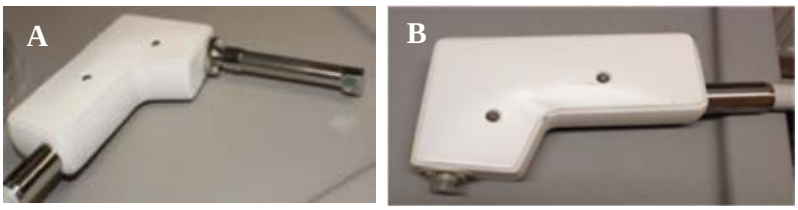

Fig. 4.

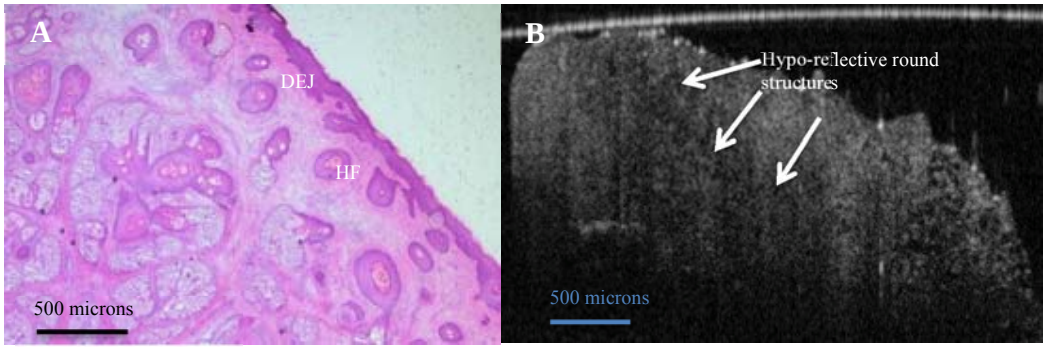

Fig. 5.

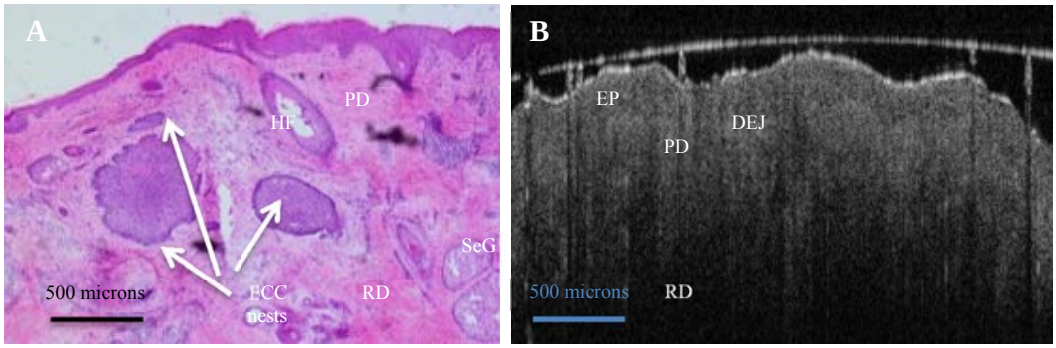

Fig. 6.

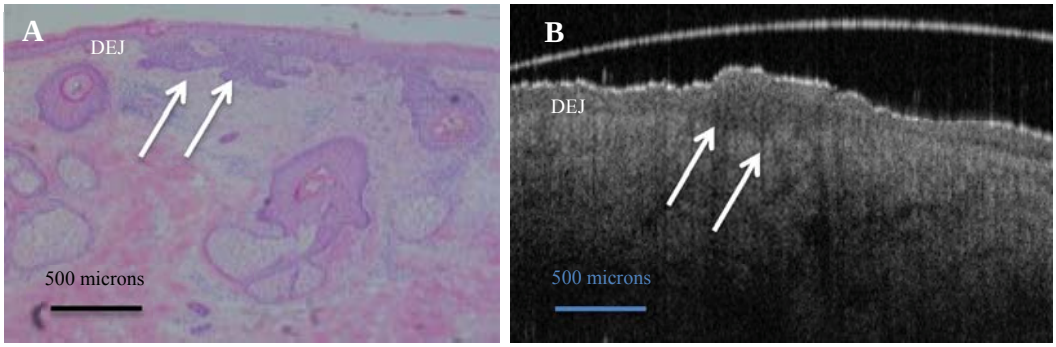

Fig. 7.

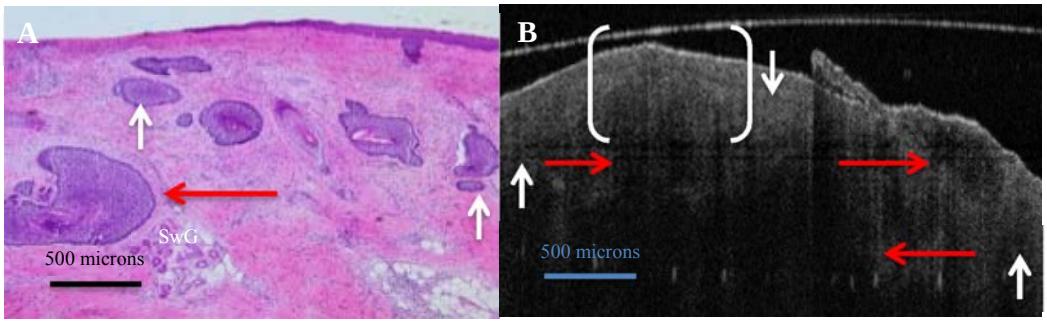

Fig. 8.

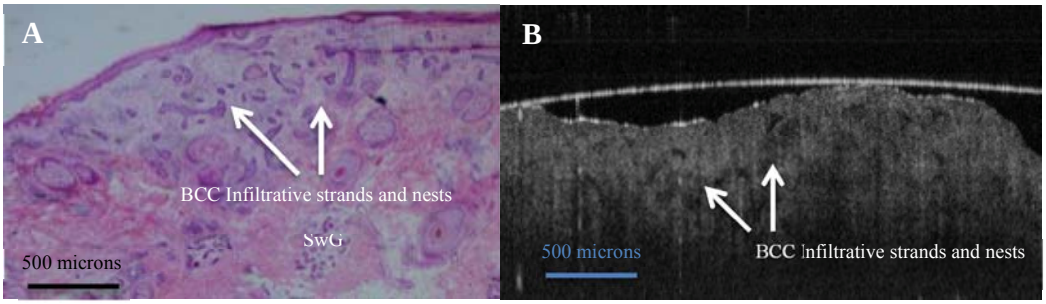

Fig. 9.

Table 1
Clinical data and BCC histopathology subtypes and location of the cohort investigated (Total 73 subjects).

Study details	No (%)
1. Gender	
Male	39 (53.5)
Female	34 (46.5)
2. Age	67.5 (range 26–96 years)
3. Location of BCC	
Cheek	17 (23.2)
Nose	17 (23.2)
Forehead/temple	14 (19.2)
Scalp	10 (13.7)
Periorbital	10 (13.7)
Ear	3 (4.2)
Lip	2 (2.8)
4. BCC subtypes	
Mixed (two or more than two subtypes)	27 (37)
Nodular	20 (27.4)
Micronodular	11 (15)
Infiltrative	8 (11)
Superficial	7 (9.6)